

SANDIA REPORT

SAND2015-10256

Unlimited Release

Printed November 2015

Test Plan for the Boiling Water Reactor Dry Cask Simulator

S.G. Durbin and E.R. Lindgren

Prepared by
Sandia National Laboratories
Albuquerque, New Mexico 87185 and Livermore, California 94550

Sandia National Laboratories is a multi-program laboratory managed and operated by Sandia Corporation, a wholly owned subsidiary of Lockheed Martin Corporation, for the U.S. Department of Energy's National Nuclear Security Administration under contract DE-AC04-94AL85000.

Approved for public release; further dissemination unlimited.



Sandia National Laboratories

Issued by Sandia National Laboratories, operated for the United States Department of Energy by Sandia Corporation.

NOTICE: This report was prepared as an account of work sponsored by an agency of the United States Government. Neither the United States Government, nor any agency thereof, nor any of their employees, nor any of their contractors, subcontractors, or their employees, make any warranty, express or implied, or assume any legal liability or responsibility for the accuracy, completeness, or usefulness of any information, apparatus, product, or process disclosed, or represent that its use would not infringe privately owned rights. Reference herein to any specific commercial product, process, or service by trade name, trademark, manufacturer, or otherwise, does not necessarily constitute or imply its endorsement, recommendation, or favoring by the United States Government, any agency thereof, or any of their contractors or subcontractors. The views and opinions expressed herein do not necessarily state or reflect those of the United States Government, any agency thereof, or any of their contractors.

Printed in the United States of America. This report has been reproduced directly from the best available copy.

Available to DOE and DOE contractors from
U.S. Department of Energy
Office of Scientific and Technical Information
P.O. Box 62
Oak Ridge, TN 37831

Telephone: (865) 576-8401
Facsimile: (865) 576-5728
E-Mail: reports@adonis.osti.gov
Online ordering: <http://www.osti.gov/bridge>

Available to the public from
U.S. Department of Commerce
National Technical Information Service
5285 Port Royal Rd.
Springfield, VA 22161

Telephone: (800) 553-6847
Facsimile: (703) 605-6900
E-Mail: orders@ntis.fedworld.gov
Online order: <http://www.ntis.gov/help/order-methods/#online>



Test Plan for the Boiling Water Reactor Dry Cask Simulator

S.G. Durbin and E.R. Lindgren
Advanced Nuclear Fuel Cycle Technologies

Sandia National Laboratories
P.O. Box 5800
Albuquerque, New Mexico 87185-MS0537

Abstract

The thermal performance of commercial nuclear spent fuel dry storage casks are evaluated through detailed numerical analysis. These modeling efforts are completed by the vendor to demonstrate performance and regulatory compliance. The calculations are then independently verified by the Nuclear Regulatory Commission (NRC). Carefully measured data sets generated from testing of full sized casks or smaller cask analogs are widely recognized as vital for validating these models. Recent advances in dry storage cask designs have significantly increased the maximum thermal load allowed in a cask in part by increasing the efficiency of internal conduction pathways and by increasing the internal convection through greater canister helium pressure. These same vertical, canistered cask systems rely on ventilation between the canister and the overpack to convect heat away from the canister to the environment for both above and belowground configurations. While several testing programs have been previously conducted, these earlier validation attempts did not capture the effects of elevated helium pressures or accurately portray the external convection of aboveground and belowground canistered dry cask systems. The purpose of the investigation described in this report is to produce a data set that can be used to test the validity of the assumptions associated with the calculations presently used to determine steady-state cladding temperatures in modern vertical, canistered dry cask systems.

The BWR cask simulator (BCS) has been designed in detail for both the aboveground and belowground venting configurations. The pressure vessel representing the canister has been designed, fabricated, and pressure tested for a maximum allowable pressure (MAWP) rating of 24 bar at 400 °C. An existing electrically heated but otherwise prototypic BWR Incoloy-clad test assembly is being deployed inside of a representative storage basket and cylindrical pressure vessel that represents the canister. The symmetric single assembly geometry with well-controlled boundary conditions simplifies interpretation of results. Various configurations of outer concentric ducting will be used to mimic conditions for above and

belowground storage configurations of vertical, dry cask systems with canisters. Radial and axial temperature profiles will be measured for a wide range of decay power and helium cask pressures. Of particular interest is the evaluation of the effect of increased helium pressure on allowable heat load and the effect of simulated wind on a simplified belowground vent configuration.

While incorporating the best available information, this test plan is subject to changes due to improved understanding from modeling or from as-built deviations to designs. As-built conditions and actual procedures will be documented in the final test report.

TABLE OF CONTENTS

ABBREVIATIONS/DEFINITIONS	VII
1 INTRODUCTION.....	1
1.1 Objective	2
1.2 Previous Studies	2
1.2.1 Small Scale, Single Assembly	2
1.2.2 Full Scale, Multi Assembly	2
1.2.3 Uniqueness of Present Test Series.....	4
2 APPARATUS	5
2.1 General Construction	5
2.2 Design of the Heated Fuel Bundle	7
2.3 Instrumentation.....	9
2.3.1 Thermocouples (TCs).....	9
2.3.2 Hotwires	18
2.3.3 Pressure and Pressure Vessel Leak Rates.....	19
2.3.4 Power Control.....	19
3 TESTING.....	23
3.1 Aboveground	23
3.1.1 Pre-Test Preparation	23
3.2 Belowground.....	24
3.2.1 Pre Test Preparation	24
3.2.2 Wind Generator	25
3.3 Test Matrix	26
4 STATUS.....	29
5 SUMMARY	31
6 REFERENCES.....	33

FIGURES

Figure 1.1	Typical vertical aboveground storage cask system.	1
Figure 1.2	Typical vertical belowground storage cask system.	1
Figure 2.1	General design details showing the plan view (upper left), the internal helium flow (lower left) and the external air flow for the above ground (middle) and below ground configurations (right).	5
Figure 2.2	Carbon steel pressure vessel.	6
Figure 2.3	CYBL facility housing the aboveground version of the BWR cask simulator. ...	7
Figure 2.4	Typical 9×9 BWR components used to construct the test assembly including top tie plate (upper left), bottom tie plate (bottom left) and channel box and spacers assembled onto the water rods (right).	8
Figure 2.5	Typical TC attachment to heater rod.	9
Figure 2.6	Experimental BWR assembly showing as-built <i>a</i>) axial and <i>b</i>) lateral thermocouple locations.	10
Figure 2.7	Definition of coordinate references in test apparatus.	11
Figure 2.8	BWR channel box showing thermocouple locations.	12
Figure 2.9	Storage basket showing thermocouple locations.	13
Figure 2.10	Pressure vessel showing thermocouple locations.	14
Figure 2.11	Ducting for aboveground configuration showing thermocouple locations.	15
Figure 2.12	Ducting for belowground configuration showing thermocouple locations.	16
Figure 2.13	Location of thermocouples for gas temperature measurements at elevations of 1.219, 2.438, 3.658 m (48, 96, and 144 in.).	17
Figure 2.14	TC elevations for the proposed TC lance.	18
Figure 2.15	Photographs of the two types of hot wire anemometer tips.	19
Figure 2.16	Power control system and test circuits.	20
Figure 2.17	Schematic of the instrumentation panel for voltage, current and power measurements.	20
Figure 3.1	Aboveground configuration showing the location of the hot wire probes.	23
Figure 3.2	Belowground configuration showing the location of the hot wire probes.	25
Figure 3.3	Wind generating machine across the inlet and outlet vents of the belowground test apparatus.	26
Figure 4.1	Carbon steel pressure vessel components freshly coated with high temperature paint.	29
Figure 4.2	Project schedule and Gantt chart.	30

TABLES

Table 2.1	Dimensions of assembly components in the 9×9 BWR.	8
Table 2.2	List of proposed equipment for power control.	21
Table 3.1	Test matrix for aboveground and belowground configurations.	27

ABBREVIATIONS/DEFINITIONS

ANSI	American National Standards Institute
BCS	BWR Cask Simulator
BWR	boiling water reactor
DAQ	data acquisition
DOE	Department of Energy
EPRI	Electric Power Research Institute
MSB	multi-assembly sealed basket
NRC	Nuclear Regulatory Commission
PID	proportional-integral-differential controller
PWR	pressurized water reactor
SCR	silicon controlled rectifier
SNF	spent nuclear fuel
SNL	Sandia National Laboratories
TC	thermocouple
VCC	ventilated concrete cask

This page intentionally blank

1 INTRODUCTION

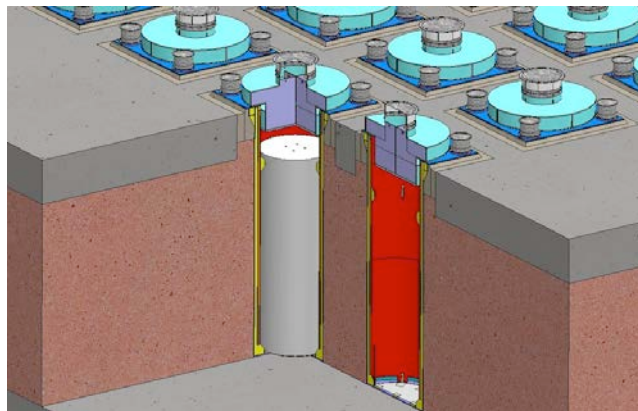
The performance of commercial nuclear spent fuel dry storage casks are typically evaluated through detailed analytical modeling of the system's thermal performance. These modeling efforts are performed by the vendor to demonstrate the performance and regulatory compliance and are independently verified by the Nuclear Regulatory Commission (NRC). The majority of commercial dry storage casks in use today are aboveground. Both horizontally and vertically oriented aboveground dry cask systems are currently in use. Figure 1.1 shows a diagram for a typical vertical aboveground system. Cooling of the assemblies located inside the sealed canister is enhanced by the induced flow of air drawn in the bottom of the cask and exiting out the top of the cask.



Source: www.nrc.gov/reading-rm/doc-collections/fact-sheets/storage-spent-fuel-fs.html

Figure 1.1 Typical vertical aboveground storage cask system.

Figure 1.2 shows a diagram for a typical, vertical belowground system. For belowground configurations air is drawn in from the top periphery and channeled to the bottom where it then flows upward along the wall of the canister and exits out the top center of the cask.



Source: www.holtecinternational.com/productsandservices/wasteandfuelmanagement/hi-storm/

Figure 1.2 Typical vertical belowground storage cask system.

Carefully measured data sets generated from testing of full sized casks or smaller cask analogs are widely recognized as vital for validating design and performance models. Numerous studies have been previously conducted [Bates, 1986; Dziadosz and Moore, 1986; Irino *et al.*, 1987; McKinnon *et al.*, 1986]. Recent advances in dry storage cask designs have significantly increased the maximum thermal load allowed in a cask in part by increasing the efficiency of internal conduction pathways and by increasing the internal convection through greater canister helium pressure. These vertical, canistered cask systems rely on ventilation between the canister and the overpack to convect heat away from the canister to the environment for both above and belowground configurations. While several testing programs have been previously conducted, these earlier validation attempts did not capture the effects of elevated helium pressures or accurately portray the external convection of aboveground and belowground canistered dry cask systems. Previous cask performance validation testing did not capture these parameters. Thus the enhanced performance of modern dry storage casks cannot be fully validated using previous studies.

1.1 Objective

The purpose of this investigation is to produce a data set that can be used to test the validity of the assumptions associated with the calculations presently used to determine steady-state cladding temperatures in modern dry casks. These calculations are used to evaluate cladding integrity throughout storage cycle.

In addition, the results generated in this test series will supplement thermal data collected as part of the High Burnup Dry Storage Cask Project [EPRI, 2014]. It is anticipated that a shortened version of the thermal lance design deployed in the Cask Project will be installed in the BCS. The installation of this lance in the BCS assembly will allow the measurement of temperatures inside of a “guide tube” structure and directly on the fuel cladding.

1.2 Previous Studies

1.2.1 Small Scale, Single Assembly

Two single assembly investigations were documented in the mid-1980s [Bates, 1986; Irino *et al.*, 1987]. Both included electrically heated 15×15 pressurized water reactor (PWR) assemblies with thermocouples installed to directly measure the surface temperature of the cladding. In Bates (1986) the electrically heated assembly was instrumented with 57 TCs distributed over 7 axial levels. In Irino *et al.* (1987) the electrically heated assembly was instrumented with 92 TCs distributed over 4 axial levels. In Bates (1986) a single irradiated 15×15 PWR assembly was also studied using 105 thermocouples distributed equally into each of the fifteen guide tubes at seven axial levels. All were limited to one atmosphere helium or air, and all imposed a constant temperature boundary condition on the outer cask wall in an attempt to achieve prototypic storage temperatures in the fuel assembly bundle.

1.2.2 Full Scale, Multi Assembly

A number of full scale multi-assembly cask studies were also documented in the mid-1980s to early 1990s, one for a BWR cask with unconsolidated fuel assemblies [McKinnon *et al.*, 1986] and the others for PWR casks with both consolidated and unconsolidated fuel [Dziadosz *et al.*, 1986; McKinnon *et al.*, 1987; Creer *et al.*, 1987; McKinnon *et al.*, 1989; McKinnon *et al.*, 1992].

Only in the most recent study was a ventilated cask design tested. In all studies the cask were studied with internal atmospheres ranging from vacuum up to 1.5 bar using air, nitrogen, or helium.

In the first study [McKinnon *et al.*, 1986], 28 or 52 BWR assemblies with a total heat load of 9 or 15 kW respectively were contained in REA 2023 prototype steel-lead-steel cask with a water-glycol neutron shield. 38 TCs were installed on the cask interior. 24 of those were installed in direct contact with the center rod in 7 assemblies at up to 7 different elevations. 12 were installed on the basket at 3 different elevations. 2 TCs were installed in direct contact with a fuel rod located on the center outer face of an assembly. The cask was tested in a vertical and horizontal orientation with atmospheres of vacuum or nitrogen at 21 psia average or helium at 22 psia average.

In the earliest full scale PWR cask study [Dziadosz *et al.*, 1986], twenty-one PWR assemblies with a total heat load of 28kW were contained in a Castor-V/21 cast iron/graphite cask with polyethylene rod neutron shielding. The interior of the cask was instrumented with sixty thermocouples deployed on ten lances located in eight guide tubes and two basket void spaces. Two of the assembly lances were installed into the center assembly. Note with the use of TC lances inside of the assembly guide tubes no direct fuel cladding temperatures were measured. The cask was tested in a vertical and horizontal orientation with atmospheres of vacuum or nitrogen at 0.57 bar or helium at 0.52 bar.

A relatively low total heat load of 12.6kW was tested in a Westinghouse MC-10 cask with 24 PWR assemblies [McKinnon *et al.*, 1987]. The MC-10 has a forged steel body and distinctive vertical carbon steel heat transfer fins around the outer circumference. The outer surface of the cask was instrumented with 34 thermocouples. The interior of the cask was instrumented with 54 thermocouples deployed on 9 TC lances in 7 fuel assembly guide tubes and 2 basket void spaces. The cask was tested in a vertical and horizontal orientation and interior atmosphere was either a vacuum or 1.5 bar helium or air.

A pair of studies using the same TN-24 cask was tested with 24 PWR assemblies with 20.5 kW total output [Creer *et al.*, 1987] or 24 consolidated fuel canisters with 23 kW total output [McKinnon *et al.*, 1989]. The TN-24P has a forged steel body surrounded by a resin layer for neutron shielding. The resin layer is covered by a smooth steel outer shell. The TN-24P is a prototype version of the standard TN-24 cask with differences in the cask body thickness, basket material and neutron shield structure. The TN-24P also incorporates 14 thermocouples into the basket structure. In both studies the fuel was instrumented with 9 TC lances with 6 TCs per lance, 7 in fuel guide tubes and 2 in simulated guide tubes in basket void spaces. The outside surface was instrumented with 35 TCs in the unconsolidated fuel study [Creer *et al.*, 1987] and 27 TCs in the consolidated fuel study [McKinnon *et al.*, 1989]. In both studies the cask was tested in a vertical and horizontal orientation with the interior atmosphere as either a vacuum or 1.5 bar helium or air. A seventh test was conducted in the consolidated fuel study [McKinnon *et al.*, 1989] for a horizontal orientation under vacuum with insulated ends to simulate impact limiters.

None of the previous studies discussed so far included or accounted for internal ventilation of the cask. Both of the single assembly investigations imposed constant temperature boundary

conditions [Bates, 1986; Irino *et al.*, 1987] and 4 full scale cask studies discussed so far [Dziadosz *et al.*, 1986; McKinnon *et al.*, 1987; Creer *et al.*, 1987; McKinnon *et al.*, 1989] considered externally cooled cask designs.

In only one previous study was a ventilated cask design considered, and this cask was the VSC-17 [McKinnon *et al.*, 1992]. The VSC-17 cask system consists of a ventilated concrete cask (VCC) and a removable multi-assembly sealed basket (MSB). The VCC is steel lined and incorporates four inlet vents to the outside near the bottom and four outlet vents near the top. When the MSB is placed inside the VCC an annular gap is formed and the vents allow air to be drawn in from the bottom through the annular gap and out the top vents. The lid on the MSB is a specially designed bolted closure that seals the basket interior and closes off the top of the cask above the top vents. The VSC-17 is a specially designed test version (holding 17 PWR assemblies) of the commercial VSC-24 cask (holding 24 PWR assemblies). The VSC-17 is smaller and lighter and incorporates the bolted lid to facilitate testing. The VSC-24 is larger and utilizes a welded lid canister for containing the spent fuel assemblies.

In the investigation of the VSC-17 cask, 17 consolidated PWR fuel canisters with a total heat load of 14.9 kW were utilized. The cask system was instrumented with 98 thermocouples. 42 of these were deployed on 7 TC lances with 6 TCs each. 6 lances were installed in the fuel canisters and one was installed in a basket void space. 9 TCs were located on the outer MSB wall and 9 TCs were located on the inner VCC liner. 10 TCs were embedded in the VCC concrete wall. One TC was located at each vent inlet and outlet. 13 TCs were located on the outer cask surface and weather cover. Testing consisted of six runs all in a vertical orientation. In 4 tests the MSB was filled with helium at an average pressure of 0.95 bar. The vents were either all unblocked, or the inlets were half blocked, or the inlets were fully blocked or both the inlets and outlets were fully blocked. The other two runs were with unblocked vents and 0.84 bar nitrogen or vacuum.

1.2.3 Uniqueness of Present Test Series

The present investigation differs in a number of significant ways. Principle among these is that the canister will accommodate helium pressures up to 24 bar at 400 °C. Additionally, ventilated design boundary conditions for aboveground and belowground configurations are explicitly considered. The experimental approach of the present study is different than the previous studies. Rather than striving to achieve prototypic peak clad temperatures by artificially imposing a temperature boundary condition on the canister wall, the present study represents the physics of near-prototypic boundary conditions.

2 APPARATUS

2.1 General Construction

The general design details are shown in Figure 2.1. An existing electrically heated but otherwise prototypic BWR Incoloy-clad test assembly will be deployed inside of a representative storage basket and cylindrical pressure vessel that represents the canister. The symmetric single assembly geometry with well-controlled boundary conditions simplifies interpretation of results. Various configurations of outer concentric ducting will be used to mimic conditions for above and belowground storage configurations of vertical, dry cask systems with canisters. Radial and axial temperature profiles will be measured for a wide range of decay power and canister helium pressures. Of particular interest is the evaluation of the effect of increased helium pressure on heat load for both the aboveground and belowground configurations. The effect of wind speed will also be measured for the belowground configuration. External mass flow rates and convective heat transfer coefficients will also be calculated from measurements of the external cooling flows.

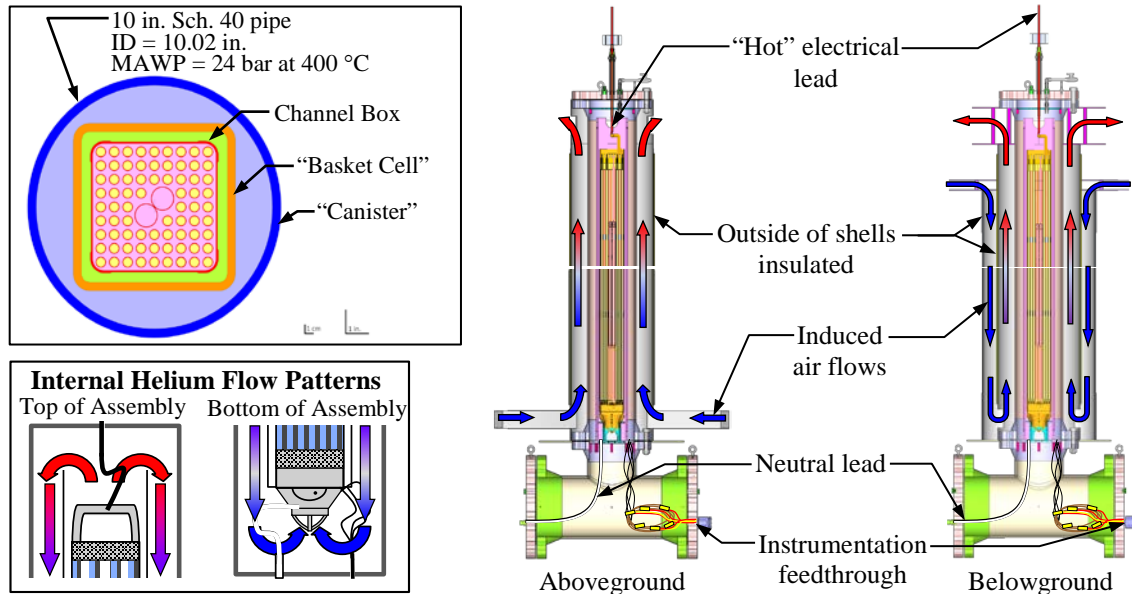


Figure 2.1 General design details showing the plan view (upper left), the internal helium flow (lower left) and the external air flow for the above ground (middle) and below ground configurations (right).

Figure 2.2 shows some of the carbon steel components used to fabricate the pressure vessel. The 4.572 m (180 in.) long vertical test section is made from 0.254 m (10 in.) Schedule 40 pipe welded to Class 300 flanges. The 0.356 × 0.254 m (14 × 10 in.) Schedule 40 reducing tee is needed to facilitate routing over 150 thermocouples (TCs) out of the pressure vessel. Blind flanges with threaded access ports for TC and power lead pass-throughs are bolted to the top of the vertical test stand section and the sides of the reducing tee. The maximum allowable working pressure is 24 bar at 400 °C. Bar stock tabs were welded inside the 0.254 m (10 in.) flange on the tee to support the test assembly and allow an insulated top boundary condition.

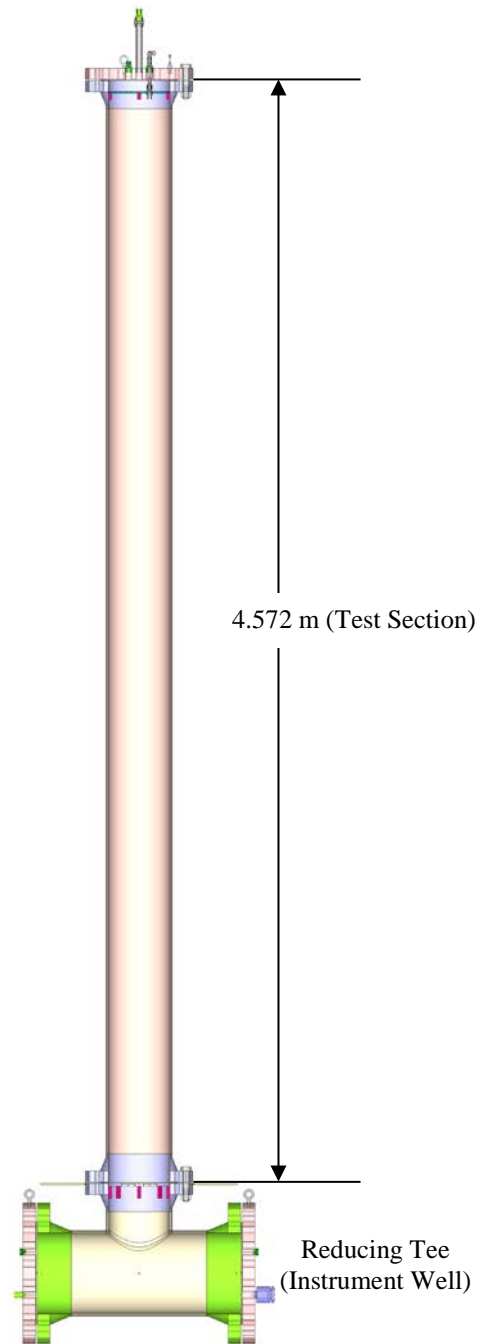


Figure 2.2 Carbon steel pressure vessel.

The test configurations will be assembled and operated inside of the Cylindrical Boiling (CYBL) test facility, which is the same facility used for earlier fuel assembly studies [Lindgren and Durbin, 2007]. CYBL is a large stainless steel containment vessel repurposed from earlier flooded containment/core retention studies sponsored by DOE. Since then CYBL has served as an excellent general-use engineered barrier for the isolation of high-energy tests. The outer vessel is 5.1 m in diameter and 8.4 m tall (16.7 ft. in diameter and 27.6 feet tall) and constructed

with 9.5 mm (0.375 in.) thick stainless steel walls. Figure 2.3 shows a scaled diagram of CYBL facility with the aboveground version of the test BCS inside.

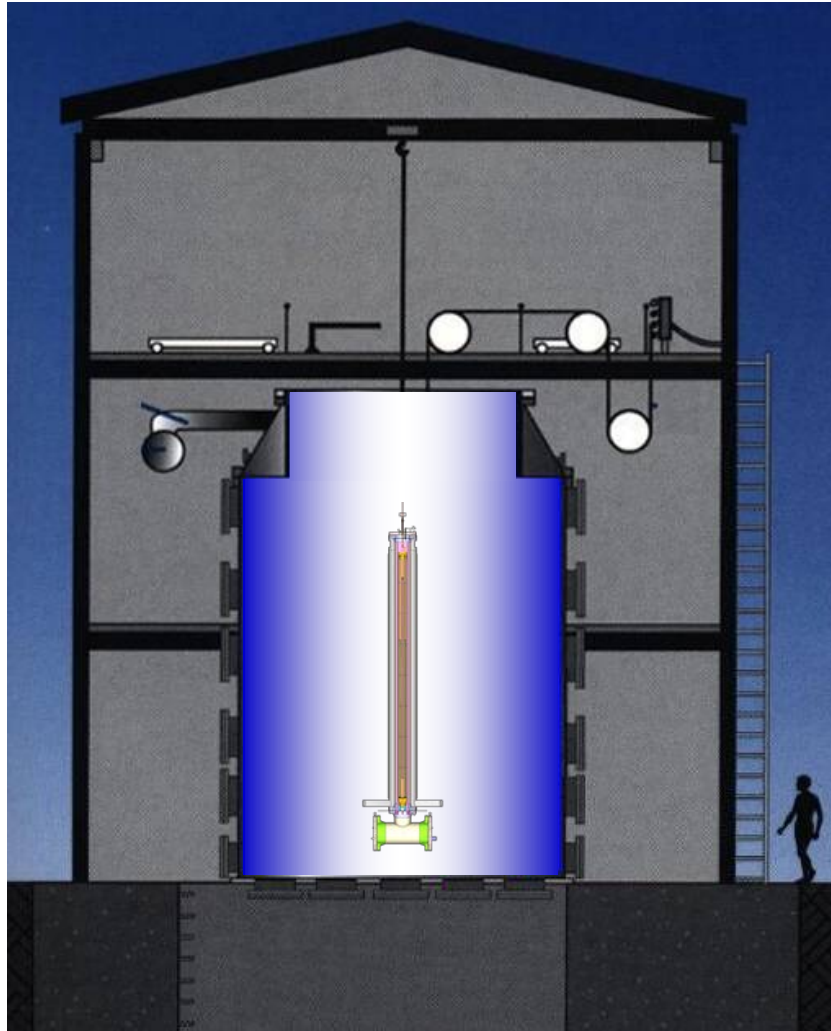


Figure 2.3 CYBL facility housing the aboveground version of the BWR cask simulator.

2.2 Design of the Heated Fuel Bundle

The highly prototypic fuel assembly was modeled after a 9×9 BWR. Commercial components were purchased to create the assembly including the top and bottom tie plates, spacers, water rods, channel box, and all related assembly hardware (see Figure 2.4). Incoloy heater rods were substituted for the fuel rod pins for heated testing. Due to fabrication constraints the diameter of the Incoloy heaters was slightly smaller than prototypic pins, 10.9 mm versus 11.2 mm. The slightly simplified Incoloy mock fuel pins were fabricated based on drawings and physical examples from the nuclear component supplier. The dimensions of the assembly components are listed below in Table 2.1.

Table 2.1 Dimensions of assembly components in the 9×9 BWR.

Description	Lower (Full) Section	Upper (Partial) Section
Number of pins	74	66
Pin diameter (mm)	10.9	10.9
Pin pitch (mm)	14.4	14.4
Pin separation (mm)	3.48	3.48
Water rod OD (main section) (mm)	24.9	24.9
Water rod ID (mm)	23.4	23.4
Nominal channel box ID (mm)	134	134
Nominal channel box OD (mm)	139	139

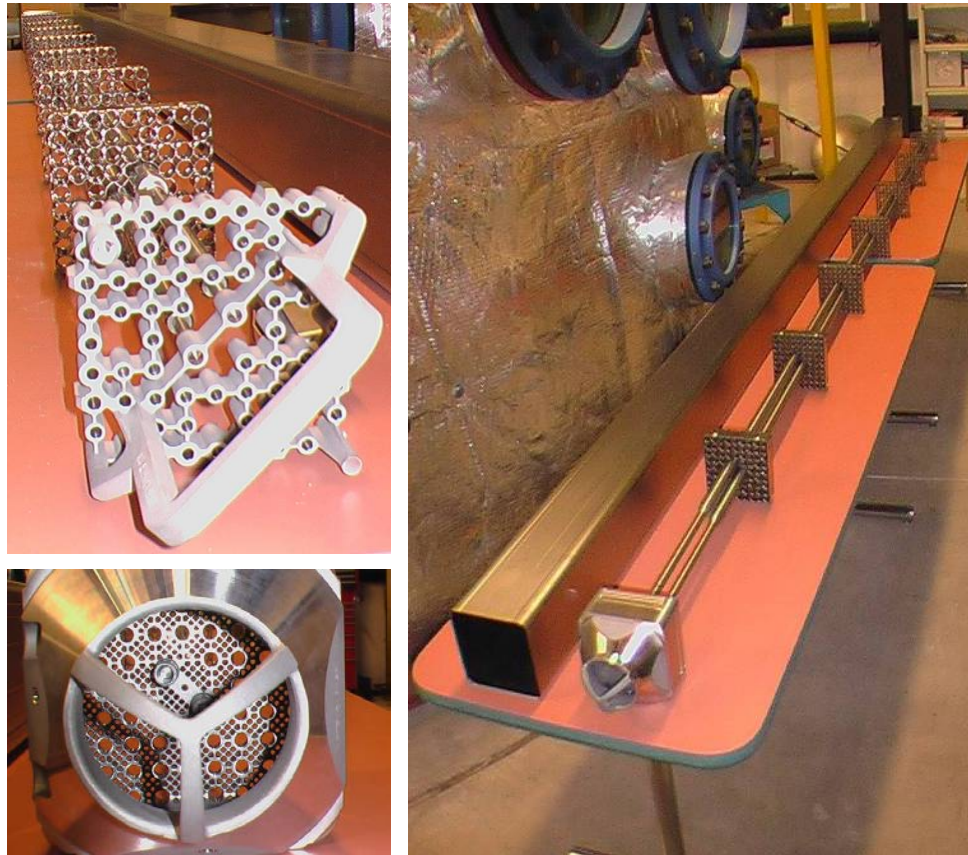


Figure 2.4 Typical 9×9 BWR components used to construct the test assembly including top tie plate (upper left), bottom tie plate (bottom left) and channel box and spacers assembled onto the water rods (right).

The thermocouples used are ungrounded junction Type K with an Incoloy sheath diameter of 0.762 mm (0.030 in.) held in intimate contact with the cladding by a thin Nichrome shim. This shim is spot welded to the cladding as shown in Figure 2.5. The TC attachment method allows the direct measurement of the cladding temperature.



Figure 2.5 Typical TC attachment to heater rod.

2.3 Instrumentation

The test apparatus will be instrumented with thermocouples (TCs) for temperature measurements, pressure transducers to monitor the internal helium pressure, and hot wire anemometers for flow velocity measurement in the exterior ducting. Volumetric flow controllers will be used to calibrate the hotwire probes. Voltage, amperage, and electrical power transducers will be used for monitoring the electrical energy input to the test assembly.

97 thermocouples are already installed on the BWR test assembly. Details of the BWR test assembly and TC locations are described elsewhere [Lindgren and Durbin, 2007]. Additional thermocouples will be installed on the other major components of the test apparatus such as the channel box, storage basket, canister wall, and exterior air ducting. TC placement on these components is designed to correspond with the existing TC placement in the BWR assembly.

Hot wire anemometers were chosen to measure the inlet flow rate because this type of instrument is sensitive and robust while introducing almost no unrecoverable flow losses. Due to the nature of the hot wire measurements, best results are achieved when the probe is placed in an isothermal, unheated gas flow. Calibration of the hot wires will be performed by imposing a known mass flow rate of air through the ducting with the hot wires in place.

2.3.1 Thermocouples (TCs)

2.3.1.1 BWR Assembly TC locations

The existing electrically heated prototypic BWR Incoloy-clad test assembly was previously instrumented with thermocouples in a layout shown in Figure 2.6. The assembly TCs are arranged in axial and radial arrays. The axial cross-section is depicted in Figure 2.6a and radial cross-sections are shown in Figure 2.6b. The axial array A1 has TCs nominally spaced every 0.152 m (6 in.) starting from the top of the bottom tie plate ($z_0 = 0$ reference plane). Axial array A2 has TCs nominally spaced every 0.305 m (12 in.) and the radial arrays are nominally spaced every 0.610 m (24 in.). The spacings are referred to as nominal due to a deviation at the 3.023

m (119 in.) elevation because of interference by a spacer. Note that the TCs in the axial array intersect with the radial arrays.

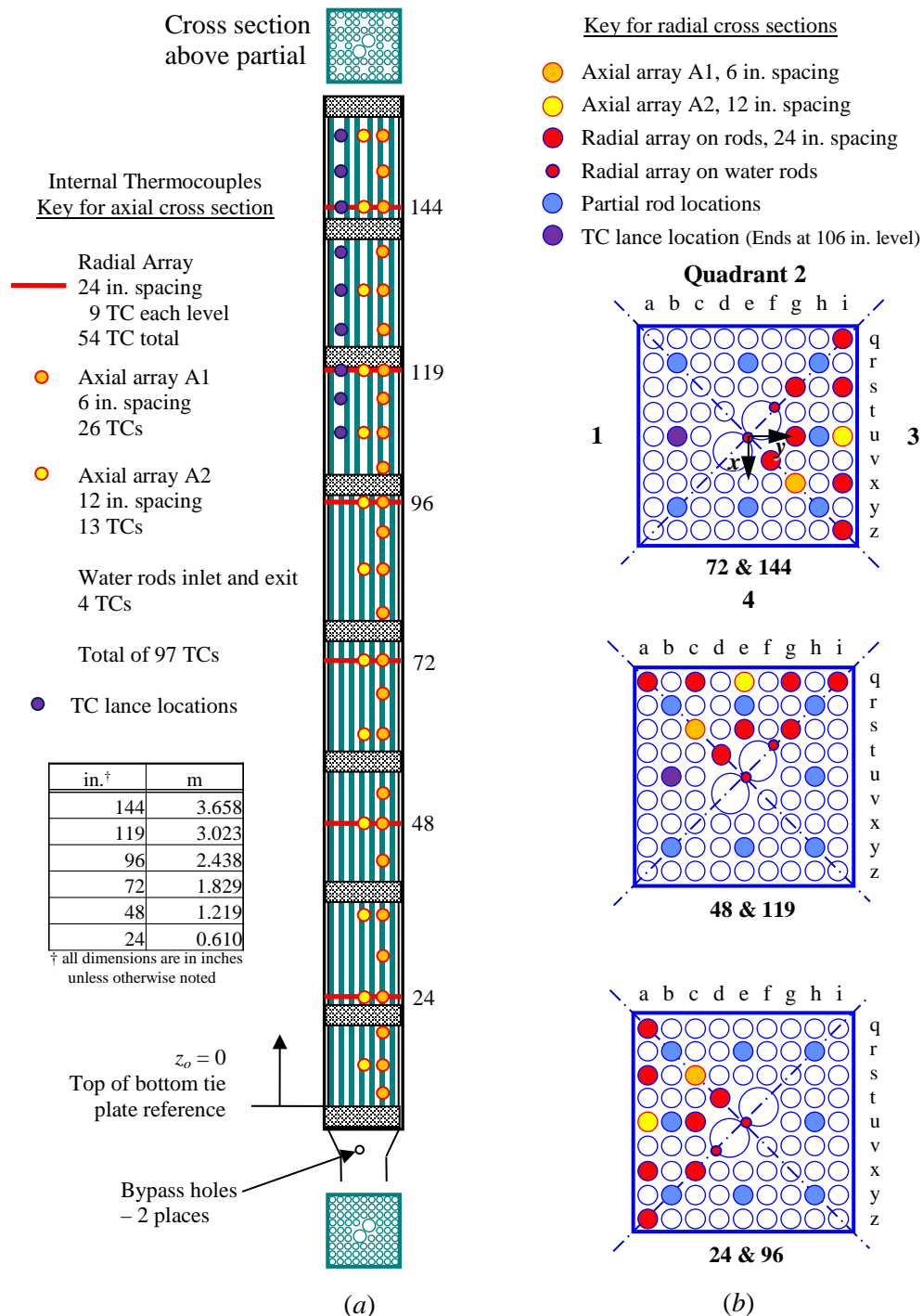


Figure 2.6 Experimental BWR assembly showing as-built *a)* axial and *b)* lateral thermocouple locations.

Based on the need to optimally balance the TC routing through the assembly the axial and radial array TCs were distributed among three separate quadrants relying on the assumption of axial symmetry.

Also shown in Figure 2.6 is the location of the proposed TC lance (for more details see Section 2.3.1.8). The quadrant for the lance deployment was chosen to minimize the possibility of damaging any of the previously installed TCs. The TC spacing on the lance will match the elevation of the TCs in the upper portion of the A1 and A2 axial arrays and the radial array at 3.023 m (119 in.) and 3.658 m (144 in.) elevations.

Figure 2.7 shows the definition of the reference coordinate system. The reference origin is defined as being in the center of the top of the bottom tie plate. The x -axis is positive in the direction of Quadrant 4 and negative in the direction of Quadrant 2. The y -axis is positive in the direction of Quadrant 3 and negative in the direction of Quadrant 1.

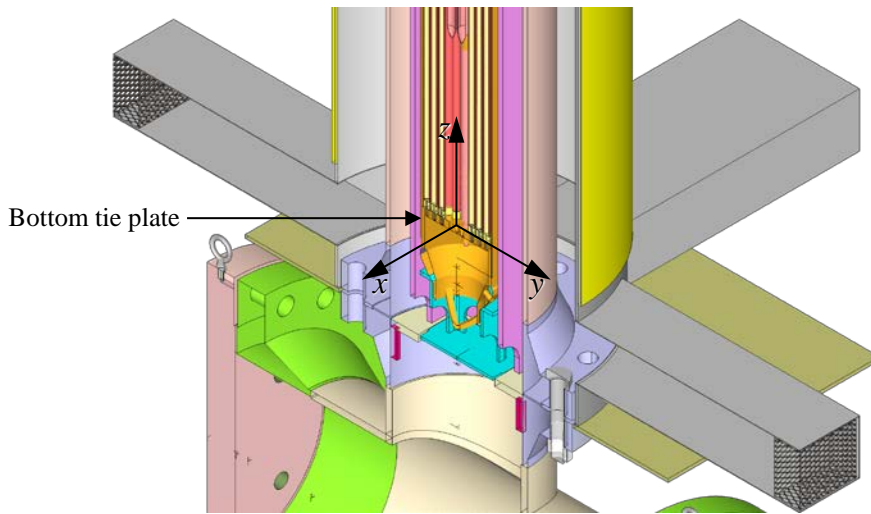


Figure 2.7 Definition of coordinate references in test apparatus.

2.3.1.2 BWR Channel Box TC Locations

The BWR channel box will be instrumented with 25 TC's as depicted in Figure 2.8. 21 of the TCs will be on the channel faces, 3 will be on the corners and one will be on the pedestal. The TCs on the faces of the channel box will be nominally located at $|x|, |y| = 0.069, 0$ m (2.704, 0 in.) or $|x|, |y| = 0, 0.069$ m (0, 2.704 in.) depending on the quadrant in which they are placed. TCs on the corners will be nominally located at $|x|, |y| = 0.065, 0.065$ m (2.564, 2.564 in.) The reference plane, z_o , is measured from the top of the bottom tie plate, the same as the BWR assembly. Multiple TCs on different faces at a given elevation will be used to check the axial symmetry assumption at 0.610 m (24 in.) intervals starting at the $z = 0.610$ m (24 in.) elevation.

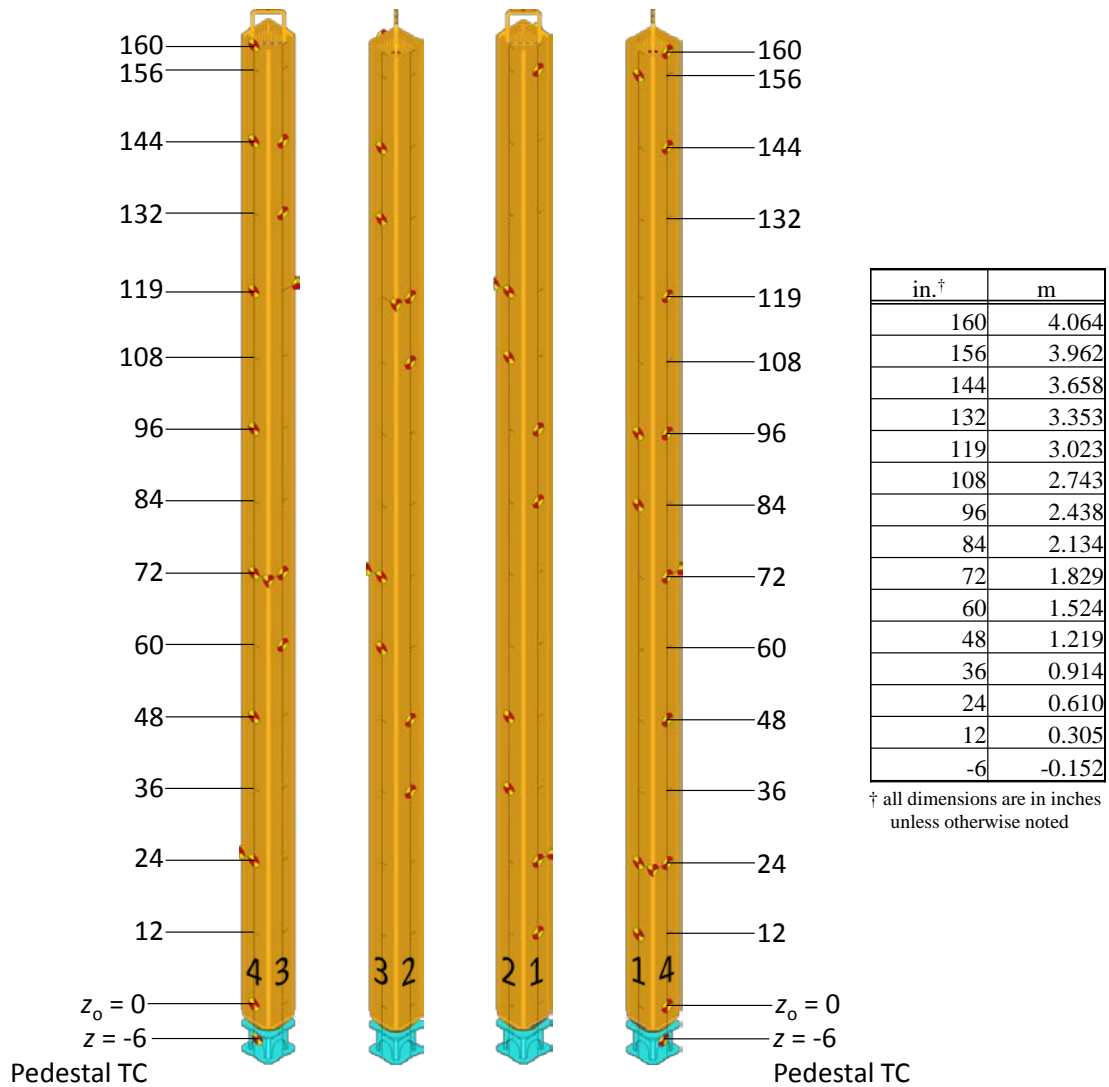


Figure 2.8 BWR channel box showing thermocouple locations.

2.3.1.3 Storage Basket TC Locations

The storage basket will be instrumented with 26 TC's as depicted in Figure 2.9. 22 of the TCs will be on the basket faces at the same positions as on the channel box, 4 will be on the corners (the corner TC at the 4.191 m (165 in.) level does not correspond to a channel box TC) and one will be on the basket face at the elevation of the pedestal. TCs located on the basket faces will be nominally located at $|x|, |y| = 0, 0.089$ m (0, 3.5 in.) and $|x|, |y| = 0.089, 0$ m (3.5, 0 in.). TCs on the corners will be nominally located at $|x|, |y| = 0.083, 0.083$ m (3.281, 3.281 in.) The reference plane, z_o , is measured from the top of the bottom tie plate.

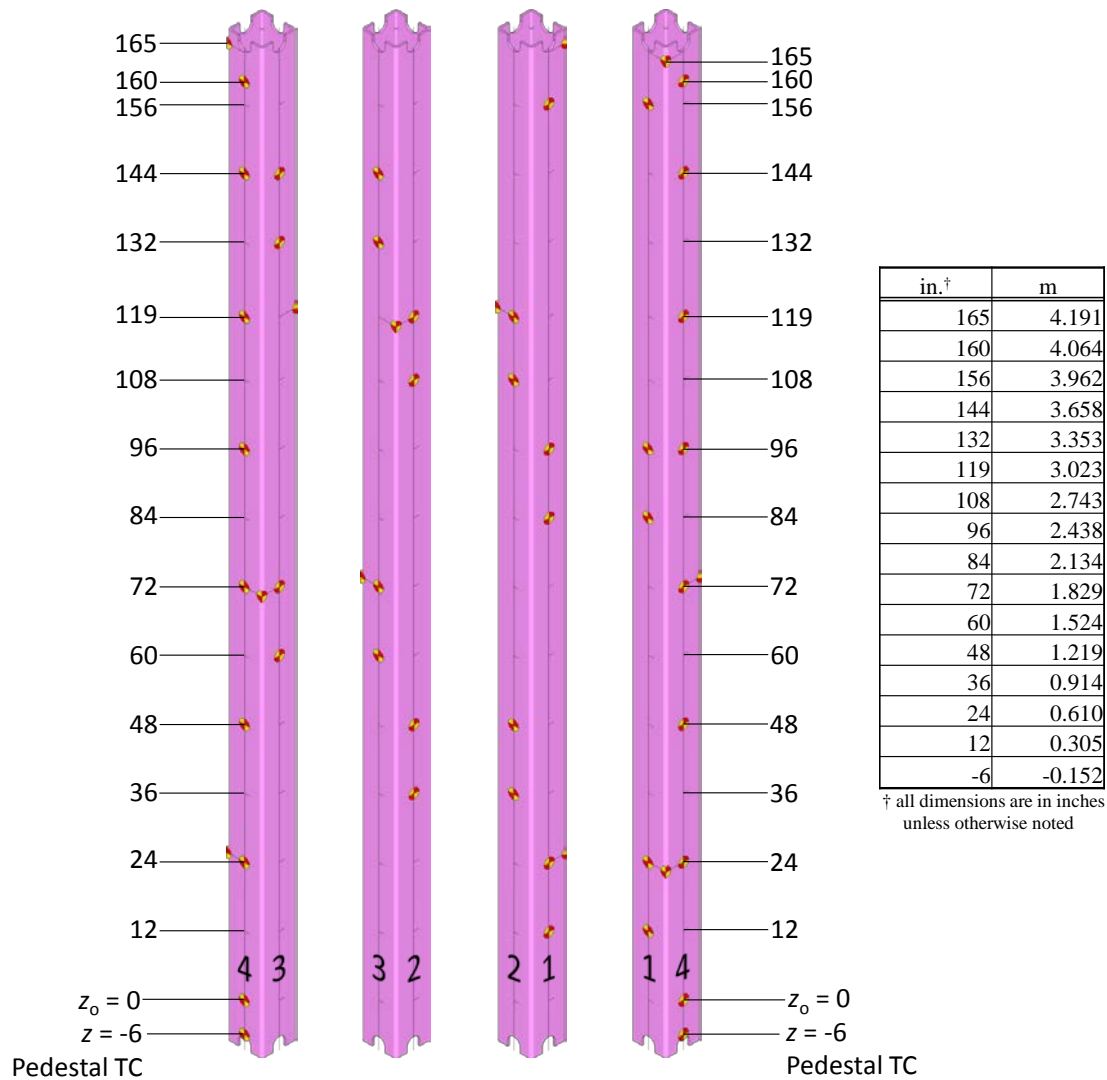


Figure 2.9 Storage basket showing thermocouple locations.

2.3.1.4 Pressure Vessel TC Locations

The pressure vessel will be instrumented with 27 TC's as depicted in Figure 2.10. 24 of the TCs will be aligned with the TCs on the storage basket faces and 3 will be aligned with the TCs on the storage basket corners. TCs aligned with the storage basket faces will be nominally located at $|x|, |y| = 0, 0.137$ m (0, 5.375 in.) and $|x|, |y| = 0.137, 0$ m (5.375, 0 in.). TCs aligned with the storage basket corners will be nominally located at $|x|, |y| = 0.097, 0.097$ m (3.801, 3.801 in.). The reference plane, z_o , is measured from the top of the bottom tie plate.

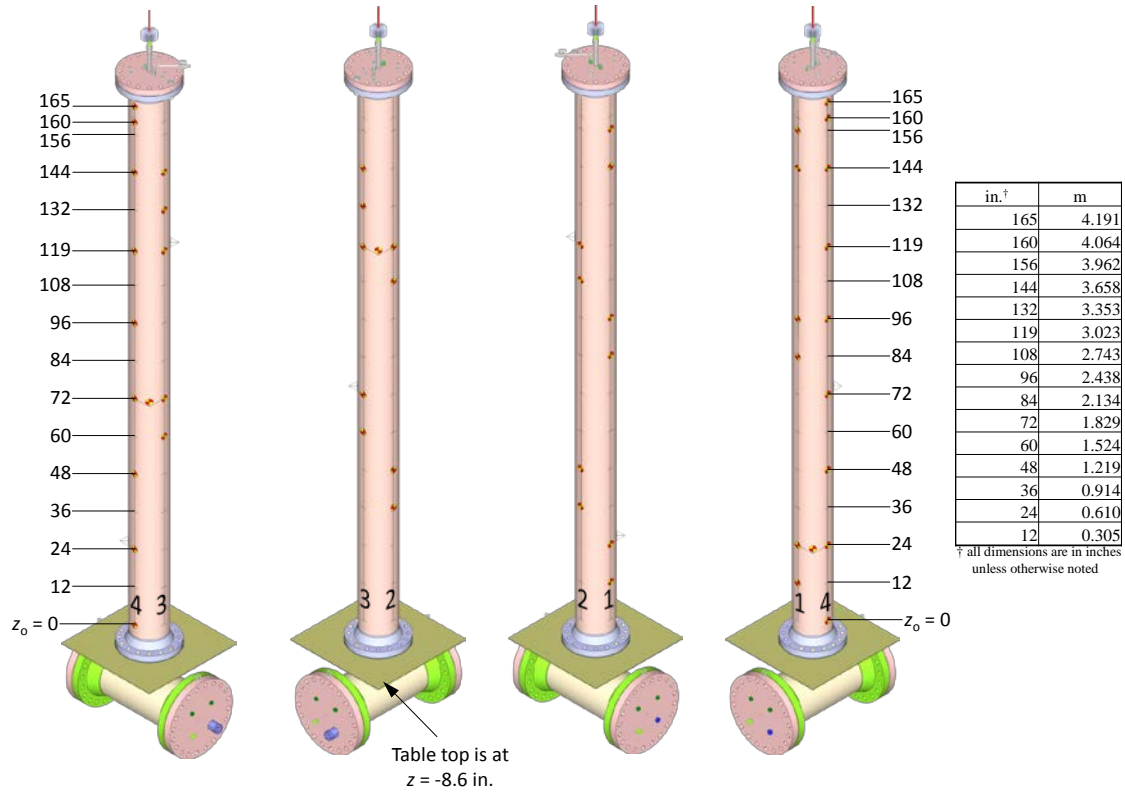


Figure 2.10 Pressure vessel showing thermocouple locations.

2.3.1.5 Aboveground Configuration Ducting TC Locations

The concentric air flow duct for the aboveground configuration will be instrumented with 27 thermocouples depicted in Figure 2.11. 24 of the TCs will be aligned with the TCs on the channel box and storage basket faces; 3 will be aligned with the corners. The face aligned TCs will be nominally located at $|x|, |y| = 0, 0.233$ m (0, 9.164 in.) and $|x|, |y| = 0.233, 0$ m (9.164, 0 in.). The corner aligned TCs will be nominally located at $|x|, |y| = 0.165, 0.165$ m (6.480, 6.480 in.). The reference plane, z_o , is measured from the top of the bottom tie plate.

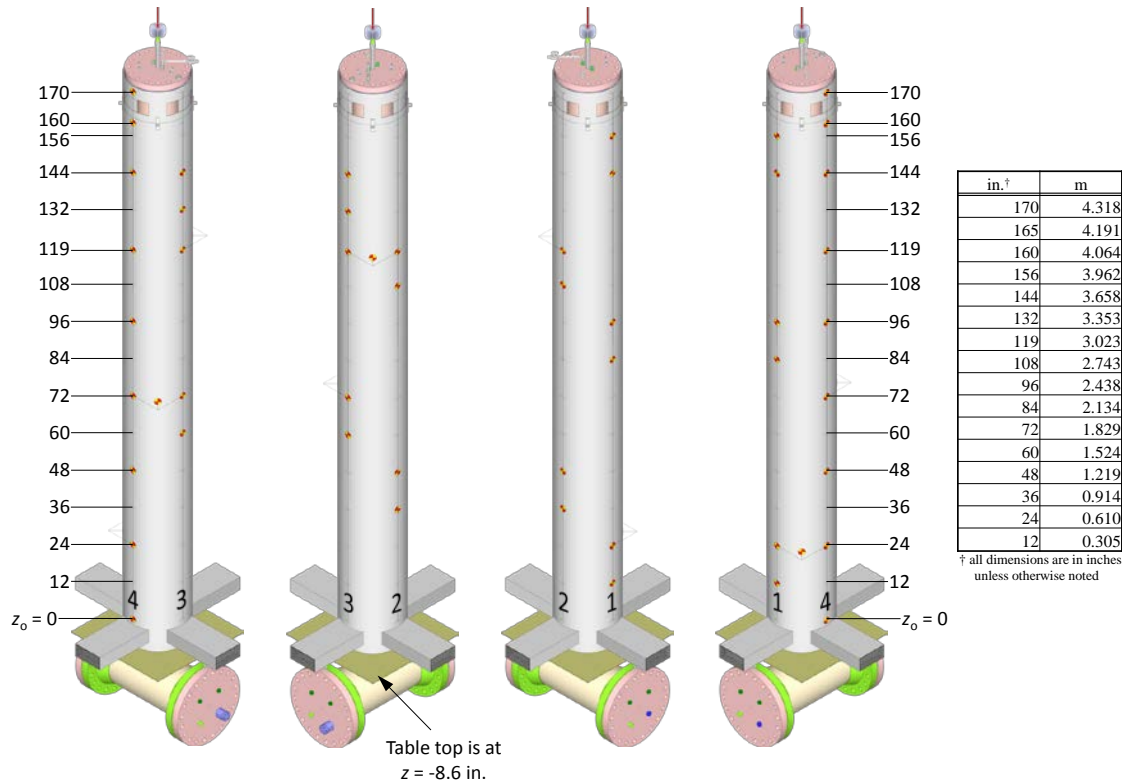


Figure 2.11 Ducting for aboveground configuration showing thermocouple locations.

2.3.1.6 Belowground Configuration Ducting TC Locations

The concentric air flow duct for the belowground configuration will be instrumented with 24 thermocouples depicted in Figure 2.12. 21 of the TCs will be aligned with the TCs on the channel box and storage basket faces; 3 will be aligned with the corners. The face aligned TCs will be nominally located at $|x|, |y| = 0, 0.316$ m (0, 12.427 in.) and $|x|, |y| = 0.316, 0$ m (12.427, 0 in.). The corner aligned TCs will be nominally located at $|x|, |y| = 0.223, 0.223$ m (8.787, 8.787 in.). The reference plane, z_o , is measured from the top of the bottom tie plate.

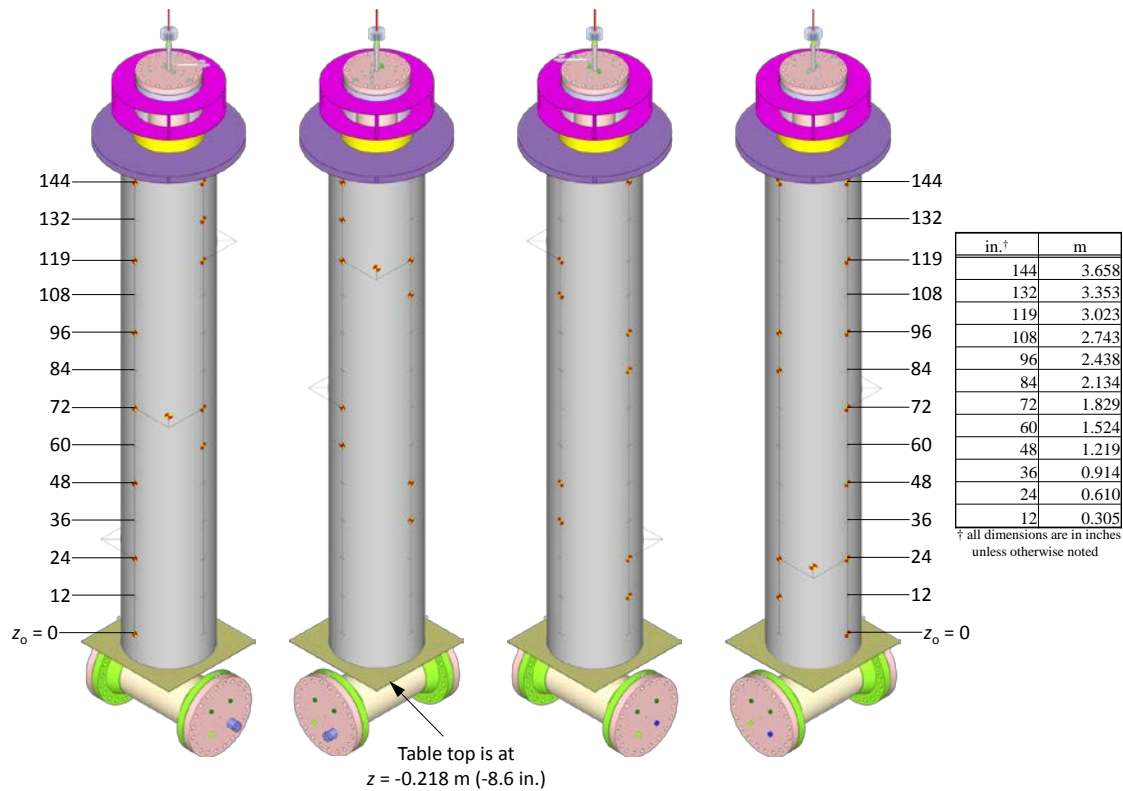


Figure 2.12 Ducting for belowground configuration showing thermocouple locations.

2.3.1.7 Gas Temperature TC Locations

Up to 37 TCs will be used to measure the temperature of the gas flowing in the various regions of the test apparatus at three different elevations as depicted in Figure 2.13 for the belowground configuration. The center region shown in red is helium flowing upward while it is heating inside the assembly and storage basket. Moving outward, the region shown in orange is helium flowing downward as it cools along the inner pressure vessel wall. A total of 17 TCs are used for gas temperature measurements inside the pressure vessel. More TCs are used at the upper two elevations where higher temperature and temperature gradients are expected.

Moving further outward the region shown in green is air moving upward as it heats along the outer pressure vessel wall. The outer most region, shown in blue, is cool air flowing downward in the belowground configuration. For the aboveground configuration, the outer blue region and the 6 TCs deployed there are absent. The narrow yellow region on the outside of each of the concentric air ducts represents a 6 mm (0.25 in.) thick layer of insulation.

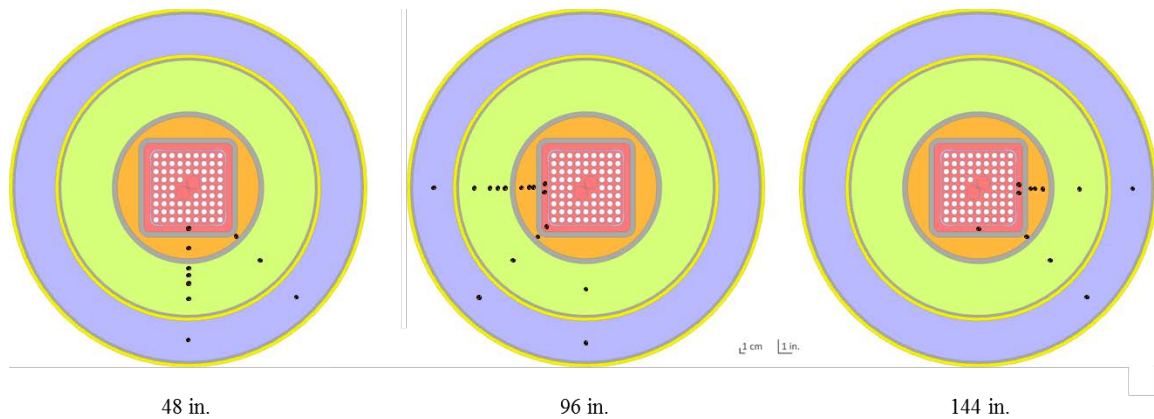


Figure 2.13 Location of thermocouples for gas temperature measurements at elevations of 1.219, 2.438, 3.658 m (48, 96, and 144 in.).

2.3.1.8 TC Lance

A custom TC lance will be deployed in the upper portion of the test assembly above a partial length rod as illustrated previously in Figure 2.6. Design details of the lance are shown in Figure 2.14. The design provides for a pressure boundary along the outer surface of the lance with a pressure seal at a penetration in the top flange using standard tube fittings. The lance will be made by the same fabricator using the same process and materials as the TC lance that will be used in the full scale High Burnup Dry Storage Cask Research and Development Project [EPRI, 2014]. The TC spacing is designed to correspond with TCs installed on the test assembly heater rod cladding as a means to provide a direct comparison between them. The direct comparison between the TC lance measurements and the corresponding clad temperature measurements is expected to aid in the interpretation of the TC lance data generated during the High Burnup Cask Project.

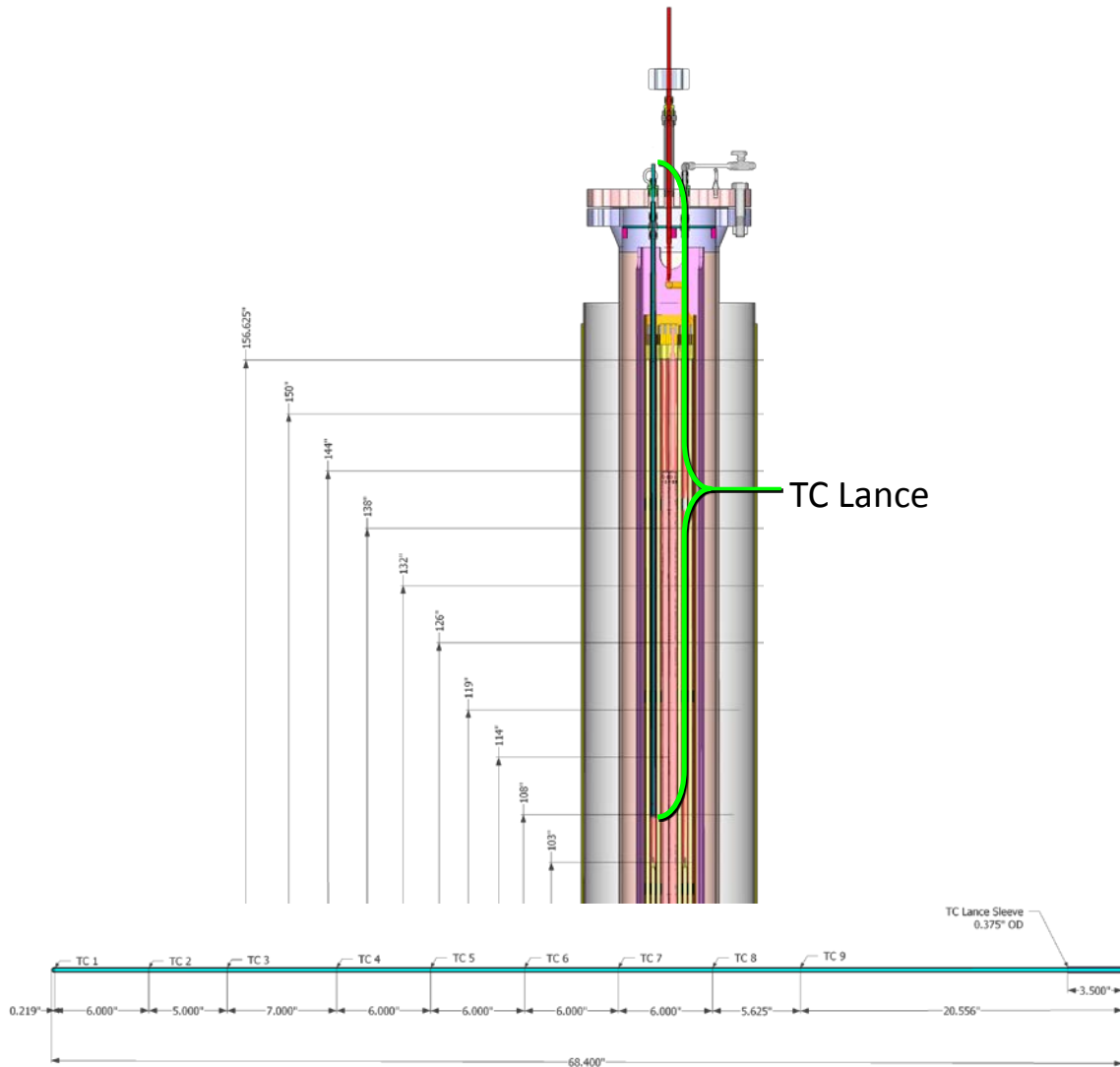


Figure 2.14 TC elevations for the proposed TC lance.

2.3.2 Hotwires

The hotwire anemometers to be used are TSI models 8475 and 8455 where the tip details are shown in Figure 2.15. For scale, the largest shaft diameter shown is 6 mm (0.25 in.). The sensing element of the model 8455 is protected inside of an open cage and is sensitive to flows down to 0.13 m/s (25 ft/min) with a fast response time of 0.2 seconds. The sensing element of the model 8475 is the ball at the tip, which results in sensitivity to flows down to 0.05 m/s (10 ft/min) but with a much larger response time of 5 seconds.



Figure 2.15 Photographs of the two types of hot wire anemometer tips.

2.3.3 Pressure and Pressure Vessel Leak Rates

Two high accuracy 0 to 500 psia absolute pressure transducers (OMEGA PX409-500A5V-XL) will be installed in the lower reducing tee. The pressure measurement is made in duplicate due of the importance of the measurement. The experimental uncertainty associated with these gauges is $\pm 0.03\%$ of full scale, or ± 0.15 psi.

A vessel with the same internal volume as the BCS (0.246 m^3 estimated) containing a single BWR fuel assembly would require a leak rate of less than $1\text{E-}4 \text{ std. cm}^3/\text{s}$ to meet the ANSI N14.5 standard for radioactive material packages [ANSI, 2014]. All penetrations and fittings currently selected for the apparatus have helium leak rates of $1\text{E-}6 \text{ std. cm}^3/\text{s}$ or better at 1 bar. In addition, spiral wound gaskets capable of leak rates of better than $1\text{E-}7 \text{ std. cm}^3/\text{s}$ will be used to form the seals at each flange. The ANSI N14.5 leak rate of $1\text{E-}4 \text{ std. cm}^3/\text{s}$ would result in an observable pressure drop of $4\text{E-}3$ psi after a one week period, which is far below the experimental uncertainty of 0.15 psi. Leaks in the as-built apparatus will be quantified as best as possible within experimental uncertainty and evaluated for possible impacts to the interpretation of any data collected.

2.3.4 Power Control

A diagram of the test assembly power control system is shown in Figure 2.16 and the details inside the Instrument Panel are shown in Figure 2.17. The electrical voltage and current delivered to the test assembly heaters is controlled to maintain a constant power by a silicon controlled rectifier (SCR). The data acquisition (DAQ) system provides a power setpoint to a PID controller that sends a control signal to the SCR based on the power measurement. The power, voltage and current measurements are collected by the DAQ. The details of the instrumentation used to control and measure the electrical power are provided in Table 2.2.

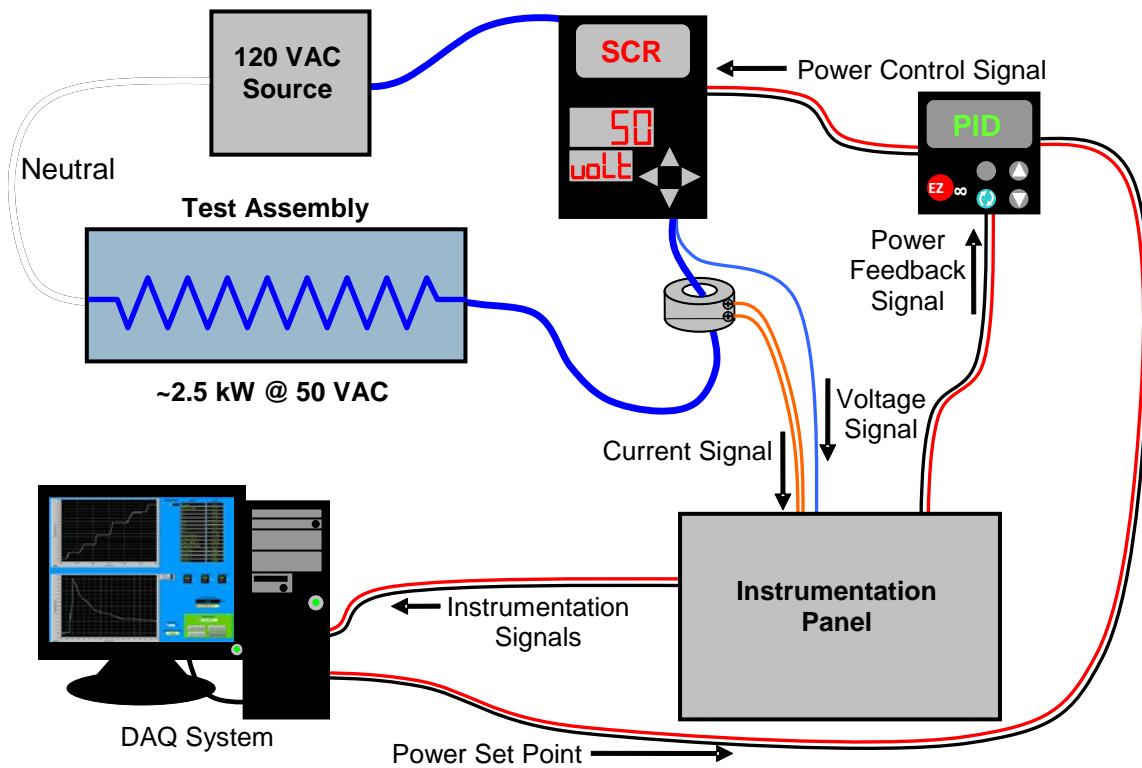


Figure 2.16 Power control system and test circuits.

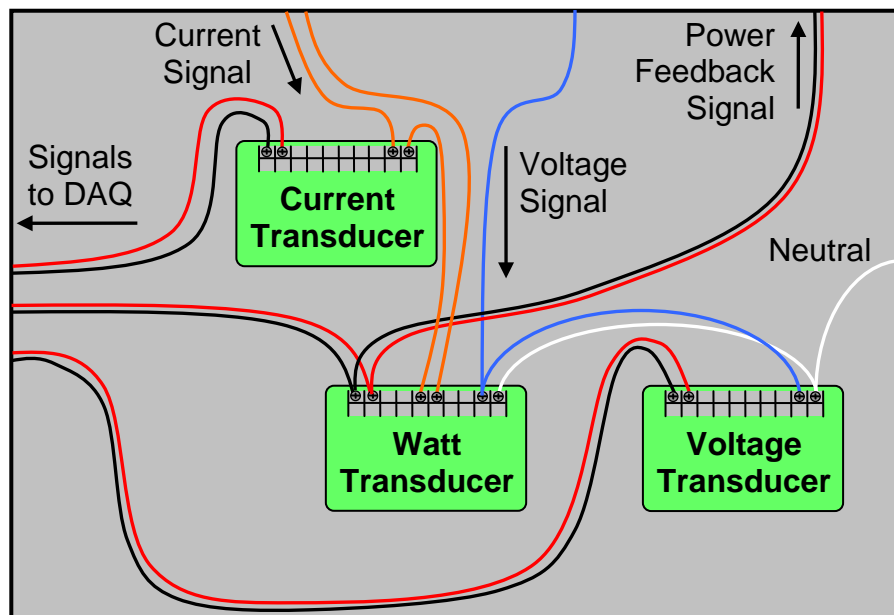


Figure 2.17 Schematic of the instrumentation panel for voltage, current and power measurements.

Table 2.2 List of proposed equipment for power control.

Description	Manufacturer	Model
AC Watt Transducer	Ohio Semitronics	PC5-001D
AC Voltage Transducer	Ohio Semitronics	3VTR-001D
AC Current Transducer	Ohio Semitronics	3CTR-010D
PID Controller	Watlow Electric Manufacturing	PM6C1FJ1RAAAAA
SCR Power Controller	Watlow Electric Manufacturing	PC91-F25A-1000

This page intentionally blank

3 TESTING

3.1 Aboveground

The inlet arrangement for the aboveground configuration is shown in Figure 3.1. Four rectangular ducts convey the inlet flow into the simulated cask. Hot wire anemometers are located in each duct and flow straightening elements at the duct entrance condition the flow.

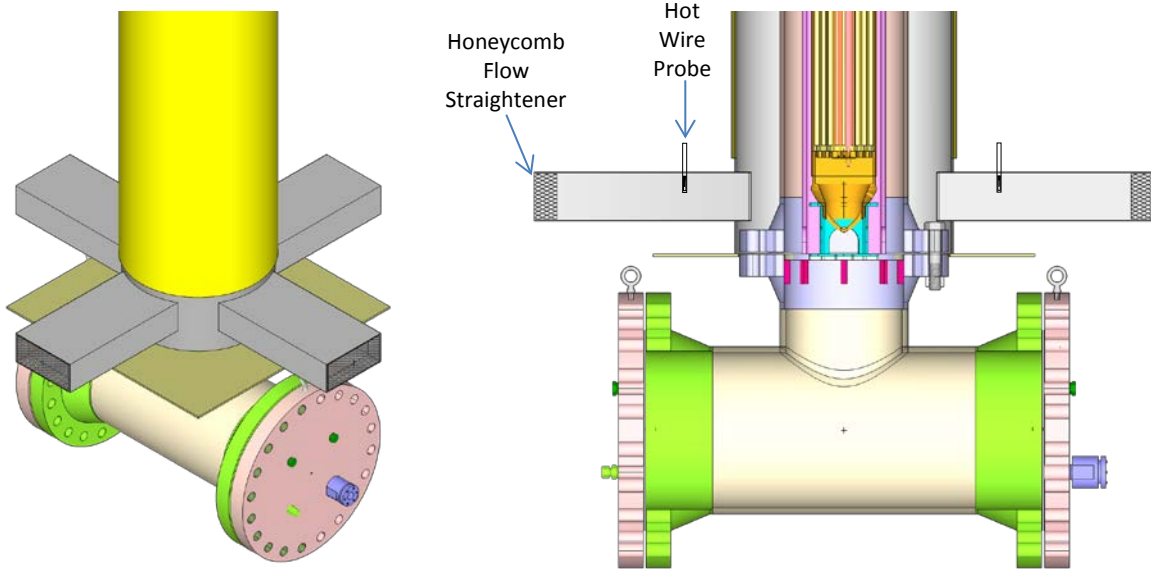


Figure 3.1 Aboveground configuration showing the location of the hot wire probes.

3.1.1 Pre-Test Preparation

3.1.1.1 Hotwire Calibrations

Hot wire anemometers were chosen to measure the inlet flow rate because this type of instrument is sensitive and robust while introducing almost no unrecoverable pressure loss. Due to the nature of the hot wire measurement, for best results the probe needs to be placed in the gas flow at the flow inlet before any gas heating has occurred and where there are minimal thermal gradients. A typical placement of the hot wire for the above ground test configuration is shown in Figure 3.1. One TSI Models 8475 and three TSI Model 8455 hot wire anemometers will be used for these tests. A honeycomb element will be added to the inlet entrance to reduce the influence of any air flow disturbances within the experimental enclosure on the hot wire measurements.

The hotwire anemometer gas flow velocity probes will be calibrated using metered forced flow. A series of unheated calibration runs will be performed to calibrate the output of the hot wire anemometer. Detailed traverses in both the horizontal and vertical direction will be made in order to provide information on the flow profile and guide finding the optimal position for the sensor. Once the optimal sensor position is determined, air flow will be metered into each of the inlet ducts individually and the response of the anemometer recorded for a range of flow rates. A least-squares regression will be used to define the linear coefficients to convert the hot wire anemometer output to a volumetric flow rate during heated testing.

3.1.1.2 Pressure Vessel Internal Volume Measurement

Before the initial fill with helium the pressure vessel will be pressurized with air in a manner that will allow the measurement of the as-built total internal volume. The pressure vessel will first be evacuated to a vacuum of 0.01 to 0.001 torr. The pressure vessel will then be slowly pressurized with a high accuracy 0 to 5 liter per minute flow controller (OMEGA FMA 2606A-TOT-HIGH ACCURACY). Two high accuracy 0 to 500 psia absolute pressure transducers (OMEGA PX409-500A5V-XL) will be used to monitor the transient fill progression. The transient mass flow and pressure data will be used to determine the total internal volume using the ideal gas law.

3.1.1.3 Initial Helium Fill

Air inside the pressure vessel will be replaced by helium by conducting successive pressurization and vent operations possibly after evacuation. Helium will be used to pressurize the vessel at ambient temperature up to 500 psia. The pressure of the vessel will be monitored for about an hour to check for leaks. If pressure drops are detected, various types of leak detectors will be used to find and repair the leak.

3.2 Belowground

Figure 3.2 shows the belowground apparatus configuration. Air is drawn into the outer duct entrance and flows downward. Insulation along the inner down comer wall prevents the air from heating. The hot wire anemometers are located in the down-comer duct at the end of the insulation near the bottom of the apparatus. The air flow turns at the bottom through the rectangular cutouts and moves upward along the hot pressure vessel wall. Hot air exits the upper central vent.

3.2.1 Pre Test Preparation

3.2.1.1 Hotwire Calibrations

Hot wire anemometers will also be used to measure the inlet flow for the belowground configuration. Due to the nature of the hot wire measurement, for best results the probe needs to be placed in the gas flow at the flow inlet before any gas heating has occurred and where there are minimal thermal gradients. The hot wire sensor placement is further complicated in the belowground configuration by the circumferentially open inlet with a contracting flow area as the inlet flow approaches the transition from horizontal radial to downward annular flow. Therefore the placement of the hot wire for the belowground test configuration will be through the outer duct wall near the bottom as shown in Figure 3.2. One TSI Models 8475 and three TSI Model 8455 hot wire anemometers will be used for these tests.

The hotwire anemometer gas flow velocity probes will be calibrated using metered forced flow. A series of unheated calibration runs will be performed to calibrate the output of the hot wire anemometer. Detailed traverses will only be possible in the horizontal radial direction. Once the optimal sensor position is determined, air flow will be metered into the single circumferential inlet and the response of all the anemometer was recorded for a range of flow rates. A least-squares regression will be used to define the linear coefficients to convert the hot wire anemometer outputs to a volumetric flow rate during heated testing.

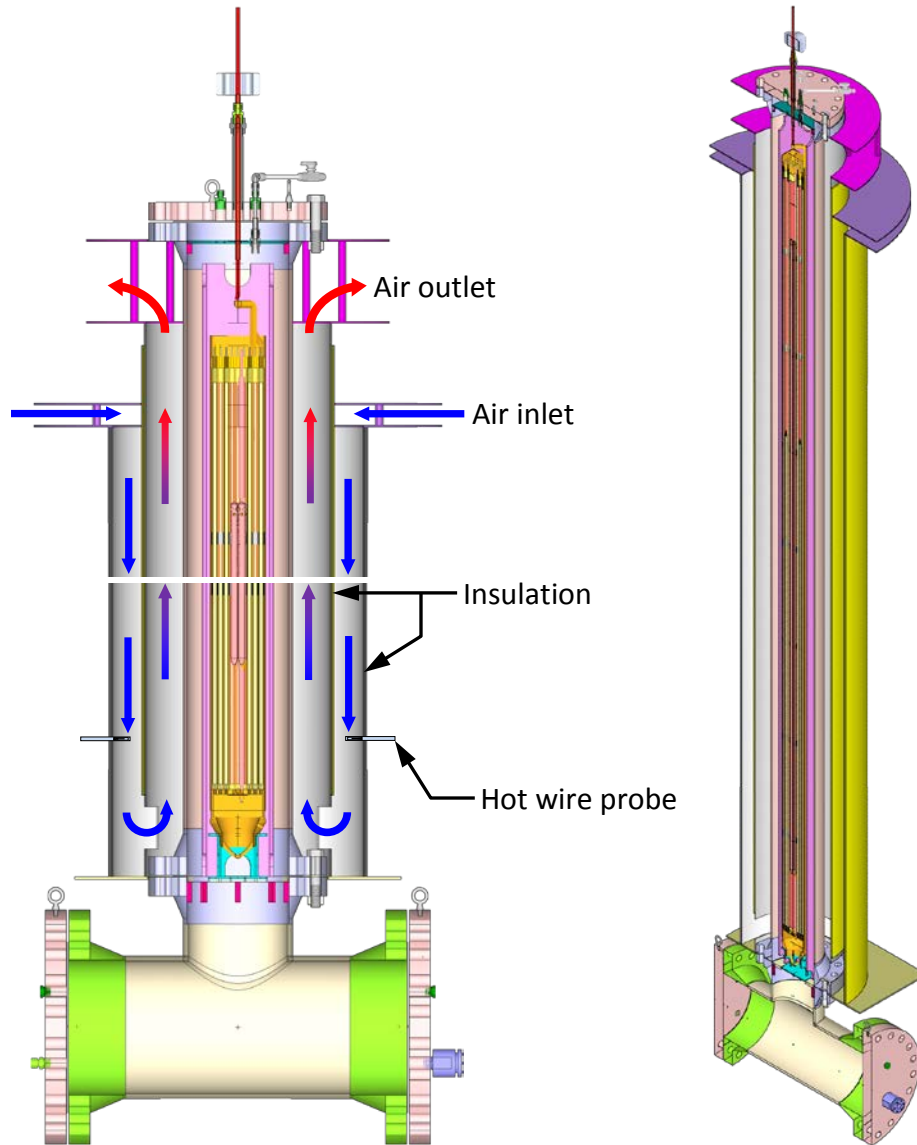


Figure 3.2 Belowground configuration showing the location of the hot wire probes.

3.2.2 Wind Generator

The effect of wind blowing across the belowground air inlet and outlet will be measured by introducing a nominally uniform velocity of air across the top of the test assembly as depicted in Figure 3.3. The current wind generator concept consists of push-pull system: a blower section and a receiver section connected by ducting. This arrangement is intended to minimize stray air currents within the CYBL vessel. The air flow is generated by three pneumatic Venturi eductors with the suction end connected to the receiving section and the outlet end ducted to the blower section. Each eductor consumes $3.54 \text{ m}^3/\text{min}$ ($125 \text{ ft}^3/\text{min}$) of compressed air to produce up to $101.4 \text{ m}^3/\text{min}$ ($3580 \text{ ft}^3/\text{min}$) of ducted air flow. Baffling and flow straightening elements in the 0.76 m (30 in.) tall by 1.22 m (48 in.) wide blower section will be implemented to produce a nominally uniform wind velocity up to 5.4 m/s (12.2 mph). CFD modeling is needed to evaluate if this type of wind machine is appropriate to simulate external wind conditions on an underground cask.

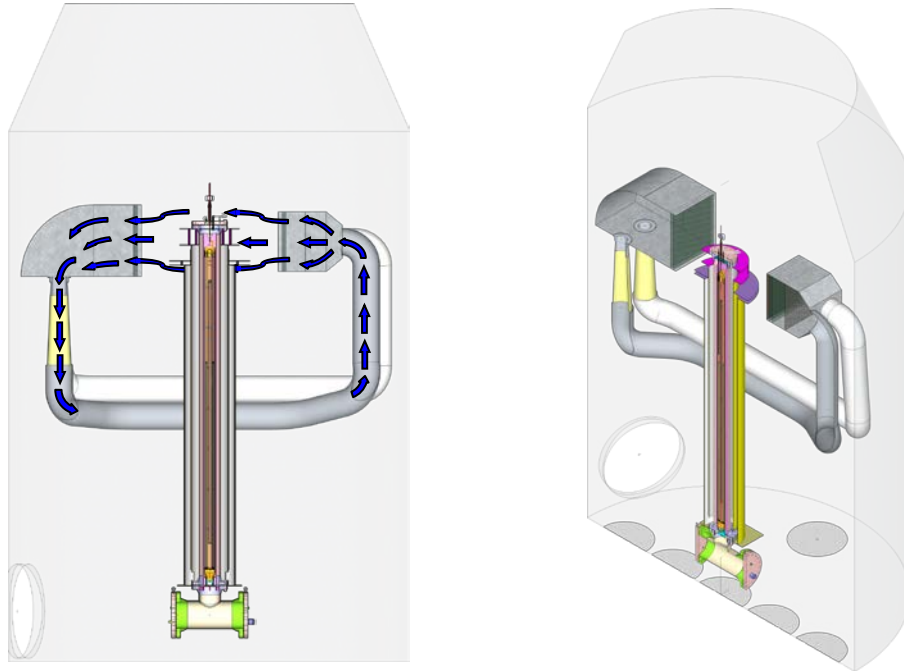


Figure 3.3 Wind generating machine across the inlet and outlet vents of the belowground test apparatus.

3.3 Test Matrix

Table 3.1 shows the test matrix. Testing will be conducted in two phases. In the first phase the experimental apparatus will be configured to represent an aboveground storage cask. Phase one testing will explore two parameters: initial helium pressure and assembly power. The pressure vessel will be filled with helium to a desired initial pressure. The test assembly will be powered at the lowest power and allowed to reach steady state. A suggested criterion for declaration of “steady state” is when the derivative of temperature with respect to time at any point within the assembly is less than 1 K/h. Based on the data collected with the BWR assembly in previous testing steady state may require 12 to 16 hours to be established.

The data collected in the last half hour represents the steady state data for that condition. After steady state has been reached for the lowest power, the power is increased to the next level and allowed to come to steady state, which may also take up to 12 h. The process is repeated for subsequent power levels. It is expected to take one work week to complete a series of three power levels for a given pressure. The vertical dashed blue arrows represent one week of testing. Two series will be conducted for the 8 bar series. One will be from 250 W to 1000 W and another from 1000 W to 2500 W. The 8 bar 1000 W case will thus be conducted to demonstrate repeatability.

Phase 2 belowground testing will explore an additional parameter of wind speed for the higher pressure cases. The low pressure series will be conducted like the Phase 1 aboveground case. For this low pressure test series, the power will be incrementally increased. For the higher pressure cases, the wind speed will be incrementally increased. For the test series with 4.5 bar helium and 500 W, the apparatus will be allowed to come to steady state first without wind. After that steady state is achieved, the wind speed will then be set to 2.25 m/s with the assembly

power kept constant. After steady state is again achieved, the wind speed will be increased again to 5 m/s. This type of test series of three steady state tests is expected to take one work week and is represented by the horizontal green dashed arrows.

CFD modeling is needed to confirm the selection of these suggested test parameters. This modeling is also required to more accurately estimate the time to achieve steady state conditions. These results will be used to plan test staffing and refine the test matrix.

Table 3.1 Test matrix for aboveground and belowground configurations.

		Belowground					
Aboveground		Wind (m/s) =>	0.0		2.25		5.0
Helium pressure (bar)	Power (W)	Helium pressure (bar)	Power (W)	Helium pressure (bar)	Power (W)	Helium pressure (bar)	Power (W)
1	500	1	500				
	1500		1500				
	2500		2500				
4.5	500	4.5	500	4.5	500	4.5	500
	1500						
	2500						
8	250	8	500	8	500	8	500
Step through powers	500						
	1000						
	1500		Step through wind speeds				
	2500						

This page intentionally blank

4 STATUS

The BCS has been designed in detail for both the aboveground and belowground venting configurations. The wind generating machine for the belowground testing has been designed. The instrumented, electrically-heated 9×9 BWR remains ready for installation. The pressure vessel that represents the canister has been designed and fabricated from carbon steel components. This vessel has been pressure tested for a MAWP rating of 24 bar at 400 °C. The carbon steel components have been painted with a high temperature paint to prevent corrosion and simulate stainless steel surface properties (see Figure 4.1).



Figure 4.1 Carbon steel pressure vessel components freshly coated with high temperature paint.

Figure 4.2 shows the project schedule and Gantt chart. Installation of the pressure vessel tee inside of the CYBL vessel and the placement of the BWR test assembly at the end of October 2015 mark the start of fabrication and setup of the aboveground configuration a few weeks ahead of schedule.

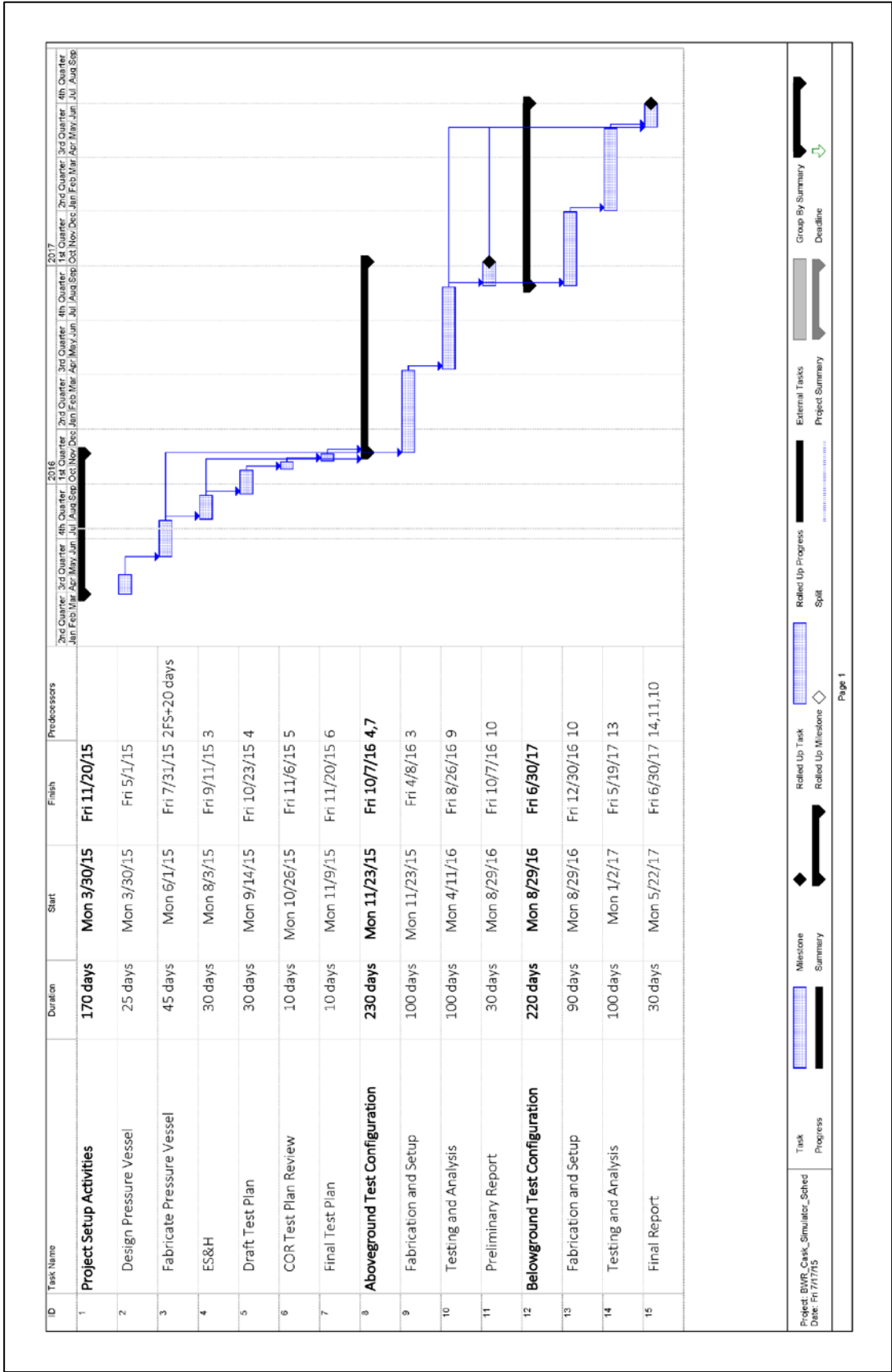


Figure 4.2 Project schedule and Gantt chart.

5 SUMMARY

The performance of commercial nuclear spent fuel dry storage casks are typically evaluated through detailed analytical modeling of the system's thermal performance. These modeling efforts are performed by the vendor to demonstrate the performance and regulatory compliance and are independently verified by the NRC. Carefully measured data sets generated from testing of full sized casks or smaller cask analogs are widely recognized as vital for validating these models. Numerous studies have been previously conducted. Recent advances in dry storage cask designs have significantly increased the maximum thermal load allowed in a cask in part by increasing the efficiency of internal conduction pathways and by increasing the internal convection through greater canister helium pressure. These vertical, canistered cask systems rely on ventilation between the canister and the overpack to convect heat away from the canister to the environment for both above and belowground configurations. While several testing programs have been previously conducted, these earlier validation attempts did not capture the effects of elevated helium pressures or accurately portray the external convection of aboveground and belowground canistered dry cask systems. Previous cask performance validation testing did not capture these parameters.

The purpose of the investigation described in this report is to produce data sets that can be used to test the validity of the assumptions associated with the calculations used to determine steady-state cladding temperatures in modern dry casks that utilize elevated helium pressure in the sealed canister or are of a design for belowground location.

An existing electrically heated but otherwise prototypic BWR Incoloy-clad test assembly is deployed inside of a representative storage basket and cylindrical pressure vessel that represents the canister. The symmetric single assembly geometry with well-controlled boundary conditions simplifies interpretation of results. Various configurations of outer concentric ducting will be used to mimic conditions for above and belowground storage configurations of vertical, dry cask systems with canisters. Radial and axial temperature profiles will be measured for a wide range of decay power and helium cask pressures. Of particular interest is the evaluation of the effect of increased helium pressure on heat load and the effect of simulated wind on the belowground vent configuration.

The BWR cask simulator has been designed in detail for both the aboveground and belowground venting configurations. The instrumented prototypic electrically heated 9×9 BWR is existing from a previous project. The pressure vessel that represents the canister has been designed, fabricated and pressure tested for a maximum allowable pressure rating of 24 bar at 400 °C.

While incorporating the best available information, this test plan is subject to changes due to improved understanding from modeling or from as-built deviations to designs. As-built conditions and actual procedures will be documented in the final test report.

This page intentionally blank

6 REFERENCES

American National Standards Institute, “American National Standard for Radioactive Materials – Leakage Tests on Packages for Shipment,” ANSI N14.5-2014, June 2014.

Bates, J.M., “Single PWR Spent Fuel Assembly Heat Transfer Data for Computer Code Evaluations,” Pacific Northwest Laboratory, PNL-5571, January 1986.

Dziadosz, D., E.V. Moore, J.M. Creer, R.A. McCann, M.A. McKinnon, J.E. Tanner, E.R. Gilbert, R.L. Goodman, D.H. Schoonen, M. Jensen, and C. Mullen, “The Castor-V/21 PWR Spent-Fuel Storage Cask: Testing and Analyses,” Electrical Power Research Institute, EPRI NP-4887, Project 2406-4, PNL-5917, UC-85, November 1986.

Electric Power Research Institute, “High Burnup Dry Storage Cask Research and Development Project: Final Test Plan,” Contract No.: DE-NE-0000593, February 2014.

Irino, M., M. Oohashi, T. Irie, and T. Nishikawa, “Study on surface temperatures of fuel pins in spent fuel dry shipping/storage casks,” IAEA-SM-286/139P, in proceedings of Packaging and Transportation of Radioactive Materials (PATRAM '86), Volume 2, p. 585, International Atomic Energy Agency Vienna, 1987.

Lindgren, E.R. and S.D. Durbin, “Characterization of Thermal-Hydraulic and Ignition Phenomena in Prototypic, Full-Length Boiling Water Reactor Spent Fuel Pool Assemblies after a Complete Loss-of-Coolant Accident”, Sandia National Laboratories, SAND2007-2270, April 2007.

McKinnon, M.A., J.W. Doman, J.E. Tanner, R.J. Guenther, J.M. Creer and C.E. King, “BWR Spent Fuel Storage Cask Performance Test, Volume 1, Cask Handling Experience and Decay Heat, Heat Transfer, and Shielding Data,” Pacific Northwest Laboratory, PNL-5777 Vol. 1, February 1986.

McKinnon, M.A., Dodge, R.E., Schmitt, R.C., Eslinger, L.E., & Dineen, G. (1992). Performance testing and analyses of the VSC-17 ventilated concrete cask (EPRI-TR--100305). United States

McKinnon, M.A., TE Michener, M.F. Jensen, G.R. Rodman, “Testing and Analyses of the TN-24P Spent Fuel Dry Storage Cask Loaded with Consolidated Fuel”, EPRI NP-6191 proj. 2813-16, PNL-6631, Feb 1989.

Creer, J.M., T.E. Michener, M.A. McKinnon, J.E. Tanner, E.R. Gilbert, R.L. Goodman, “The TN-24P PWR Spent Fuel Storage Cask: Testing and Analyses”, EPRI NP-5128 proj. 2406-4, PNL-6054, Apr. 1987.

McKinnon, M.A., J.M. Creer, C. L. Wheeler, J.E. Tanner, E.R. Gilbert, R.L. Goodman, D.P. Batala, D.A. Dziadosz, E.V. Moore, D.H. Schoonen, M.F. Jensen, and J.H. Browder, . “The MC-10 PWR Spent Fuel Storage Cask : Testing and Analysis“, Palo Alto, California : Electric Power Research Institute, July 1987. EPRI NP-5268.

DISTRIBUTION

Sandia Internal:

6223	MS0747	Samuel Durbin (3)
6223	MS0747	Eric Lindgren
9532	MS0899	Technical Library (electronic copy)

